

Article

An In-Situ Geotextile Filtration Method for Suspended Solids Attenuation and Algae Suppression in a Canadian Eutrophic Lake

Antônio Cavalcante Pereira ¹, Catherine N. Mulligan ^{1,*}, Dileep Palakkeel Veetil ¹ and Sam Bhat ²

¹ Department of Building, Civil and Environmental Engineering, Concordia University, Montréal, QC H3G 1M8, Canada

² Titan Environmental Containment Ltd., Ile des Chênes, MB R0A 0T1, Canada

* Correspondence: mulligan@civil.concordia.ca

Abstract: Climate change and human actions will exacerbate eutrophication cases in inland waters. By external or internal inputs, there will be an increase in nutrient concentrations in those systems worldwide. Those nutrients will bring faster trophic changes to inland waters and possible health and recreational advisories. A novel approach using a floating filtration system, a silt curtain, and geotextiles (woven and non-woven) is under investigation. This method has been applied as an in-situ pilot experiment deployed at Lake Caron, a shallow eutrophic lake in Quebec, for two summers. Turbidity, total suspended solids (TSS), total phosphorus (TP), blue-green-algae-phyococyanin (BGA-PC) and chlorophyll-a showed statistically significant average removal efficiencies of 53%, 22%, 49%, 57% and 56%, respectively, in the first year and 17%, 36%, 18%, 34% and 32% in the second. Statistical correlations were found with TSS, turbidity and variables that could represent particles (TP, turbidity, chlorophyll-a). Employing this in situ management method could be a promising remediation for not only shallow lakes (average depth < 2 m) but also for ponds, rivers, coastal regions, bays and other water types, to enable cleaner water for future generations.

Keywords: eutrophication; total phosphorus; algae; cyanobacteria; suspended solids; woven geotextile; lake water; remediation; surface water



Citation: Pereira, A.C.; Mulligan, C.N.; Veetil, D.P.; Bhat, S. An In-Situ Geotextile Filtration Method for Suspended Solids Attenuation and Algae Suppression in a Canadian Eutrophic Lake. *Water* **2023**, *15*, 441. <https://doi.org/10.3390/w15030441>

Academic Editor: Rolf D. Vogt

Received: 29 December 2022

Revised: 17 January 2023

Accepted: 18 January 2023

Published: 22 January 2023



Copyright: © 2023 by the authors. Licensee MDPI, Basel, Switzerland. This article is an open access article distributed under the terms and conditions of the Creative Commons Attribution (CC BY) license (<https://creativecommons.org/licenses/by/4.0/>).

1. Introduction

Pressure on inland waters, more precisely on lakes, is expected to be increasing soon due to human actions and new climate change scenarios [1–3]. Issues triggered by those new variables or mechanisms will age lakes more quickly and will bring potential recreational and drinking advisories due to high phytoplankton productivity (i.e., cyanobacteria and algae) along with harmful toxin production [4,5]. Additionally, in some cases, lake anoxia, lake volume reduction [6] and lake browning will occur [7–9].

Actual driving forces for this succession and eutrophication are expected to be exacerbated by extreme weather events [10–12]. In other words, not only events such as storms, record-breaking rainfall events, heat waves, prolonged droughts, tropical cyclones and hydrological manipulation of waterbodies but also land-use changes, deforestation and fertilizer (over)use will probably produce more eutrophic waters than before.

Those processes will increase organic matter input from point and non-point sources within inland waters by catchments (e.g., watershed runoff after increased precipitation) [13–15] and increased internal nutrient lake release due to lake warming [2,3], physical mixing of the water column and sediment resuspension. Higher organic matter presence due to degradation [16,17], and increased input by human activities (e.g., sewage discharge and fertilizer/detergent use) will be observed as well [1].

In the rising nutrient pool mentioned within lake ecosystems, phosphorus is often the limiting nutrient related to trophic level changes and a determinant factor for eutrophication [18,19] while nitrogen may be retained or lost to the atmosphere in gaseous forms by

denitrification (e.g., N_2 , NH_3 , N_2O) in shallow lake systems, due to higher sediment area to water volume ratios [20,21].

Furthermore, the phosphorus form found in the lake water column is crucial. While phosphorus from catchments is partly in the particulate form that possibly settles in the water column and is only used by phytoplankton if released [16,22], internal loads in lakes are predominantly in the dissolved form directly and bioavailable for algal/cyanobacteria growth [23]. As a result, it is compulsory to propose removal methods for external and internal phosphorus loads exacerbated in lakes due to climate change and human actions, a challenge to be achieved by nations in 2030 as described in SDG 6 (Sustainable Development Goals) (i.e., clean water and sanitation) of the UN (United Nations) agenda.

Numerous remediation methodologies are used such as hypolimnetic aeration [24,25], sediment dredging [26] lanthanum-modified bentonite addition [27,28], cement addition [29], and aluminum addition [30,31]. These remediation approaches can adversely affect the lake biota in the water column and in some cases are very costly [32]. It can also reduce the lake volume, in the case of additives or sorbents and should not be the first go-to option for an in-situ remedial.

Consequently, in-lake non-invasive and sustainable remediation techniques need to be investigated and proposed. These in-situ methods should be effective in reducing those nutrients, if possible, for the entire recreational season, be environmentally safe, relatively easy to apply and should not be too expensive [33]. With this understanding, geotextiles have been employed as membranes for inland water remediation for particulate nutrient and suspended solids attenuation by filtration [34–36], indicating their strong potential as a flexible, potentially economical, and effective environmental remediation that can be implemented at shallow lakes and other surface waters.

To this date, there are no similar in-situ treatments being proposed for the remediation of lake water. This in-situ pilot experiment was evaluated for remediating the surface water quality of the study's shallow eutrophic lake, Lake Caron. It uses custom-made woven and non-woven geotextiles as filter media in an active floating filtration unit directly deployed inside a turbidity curtain enclosed area. By removing suspended solids, it is hypothesized that an indirect reduction in nutrient availability can be achieved. Consequently, this decreases the eutrophication likelihood and suppresses algal/cyanobacteria blooms in an environmentally safe way. Thus, the main objectives of this study are to evaluate the performance of the systems for improvement of lake water quality, over the two summers' deployment (i.e., summer 2019 and summer 2020). The first was a 69-day experiment deployment and the second of 76-days. Additionally, a better understanding and potential applicability and challenges for inland water eco remediation was obtained for this method.

2. Materials and Methods

2.1. Study Area

The present study focused on improving a portion of the Lake Caron water quality ($45^{\circ}50'28''$ N; $74^{\circ}08'50''$ W) over two consecutive summers, a shallow eutrophic lake located in the Sainte-Anne des-Lacs municipality in Québec situated around 75 km north from downtown Montréal in the Laurentian Mountains. The lake is located in the Lac Ouimet watershed mainly occupied by trees and a few residents [37], represented in a graphic map in Figure 1 with sampling stations and households. In Figure 1, station D specifies the experiment deployment location (with inset map on right), and Station S is related to the sampling location similar to the Quebec Réseau de Surveillance Volontaire des Lacs (RSVL) provincial location to follow lake water quality. In the project, field sampling was performed throughout the entire lake at the six selected stations: St. S, St. 1, St. 4, St. 7, St. 8 and St. 9 over the summers of 2019 and 2020.

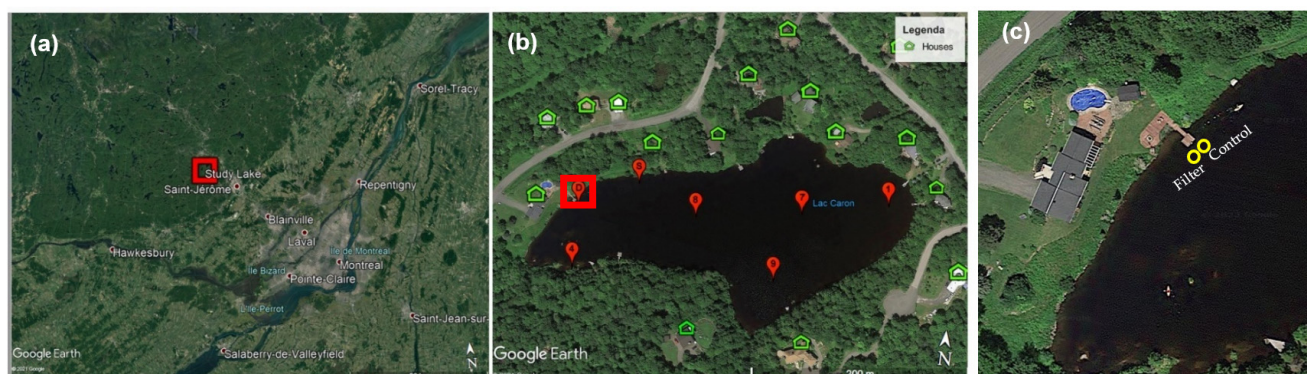


Figure 1. Regional map (a) and inset of the Lake Caron map with sampling stations (b) with an inset of the experiment approximate locations (c).

Lake Caron has maximum, minimum and average depths of 2.6, 0.5 and 1.4 m, respectively, and approximate surface area and water volume of 35,300 m² and 48,400 m³ [38]. The average annual temperature of Sainte-Anne des-Lacs is 2.6 °C (−20–24 °C), and the average annual precipitation is 1039.2 mm.

Phosphorus loadings in the lake could be linked to possible septic tank discharges and plant decomposition in the water related to external loads. In the past, the lake was enlarged by tree cutting and subsequently the decomposing stumps. In addition, phosphorus sediment release and algal decease/decomposition could be associated with internal loads. Sediment P concentration varied between 866 and 1298 mg/kg in this lake, and relatively high P concentrations are found in the sediments from St. 4 and St. 8 [34]. These are possible recurring reasons causing for algal/cyanobacteria biomass growth, every summer since 2008, which has placed this lake on a swimming advisory. Together with the MELCC (*Ministère de l'Environnement et de la Lutte Contre les Changements Climatiques*) 2018 report [39], under the Quebec Réseau de Surveillance Volontaire des Lacs (RSVL) adoption of measures to limit nutrient inputs for avoiding further degradation and loss of use is recommended.

2.2. In Situ Floating Geotextile Filtration Setup

The floating filtration equipment used in this experiment was made of Plexiglas. Material and type of unit have been selected to offer easy follow-up of geotextile clogging rate and filter media modifications. The open square filtration unit had the following dimensions of 30.5 × 30.5 × 20 cm (W × L × H) coupled with a base galvanized copper grid to support the filters; Figure 2 shows the unit with details. Additionally, a Plexiglass wall of 20 cm in height fixed by clamps was introduced for avoiding filter layer movement when the experiment is being deployed. No modifications to the filtration unit were complete throughout the two-summer experiment.

The whole unit was tied up and floated with the support of an inflated synthetic rubber tube. Figure 3 gives a representation of the in-situ deployment. Additionally, for water recirculation on the filters, two submersible water pumps (DC 12 V, 4.8 W) with flow rates of 240 L/h were used for pumping. The nearest outlet present provided the electrical supply. Additionally, a plastic prefilter was used to guarantee larger debris removal, if presented in the water as well as to guarantee that the pumped water was uniformly distributed in the geotextile. All treated water was returned to the enclosed area and the filtration unit was able to move freely inside the contained water during the experiment duration.

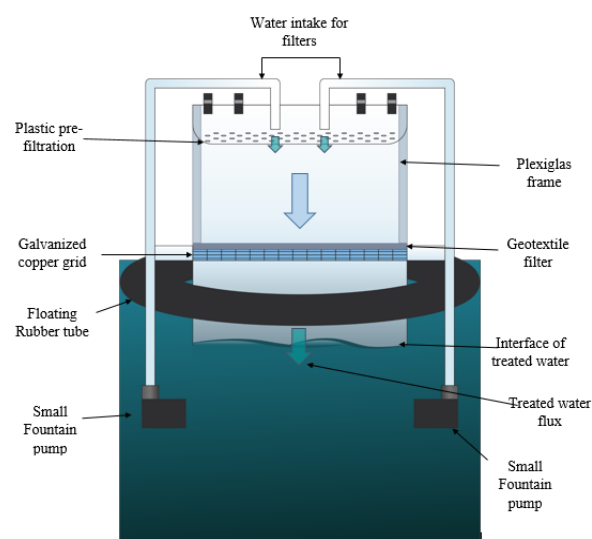


Figure 2. Floating filtration unit components.

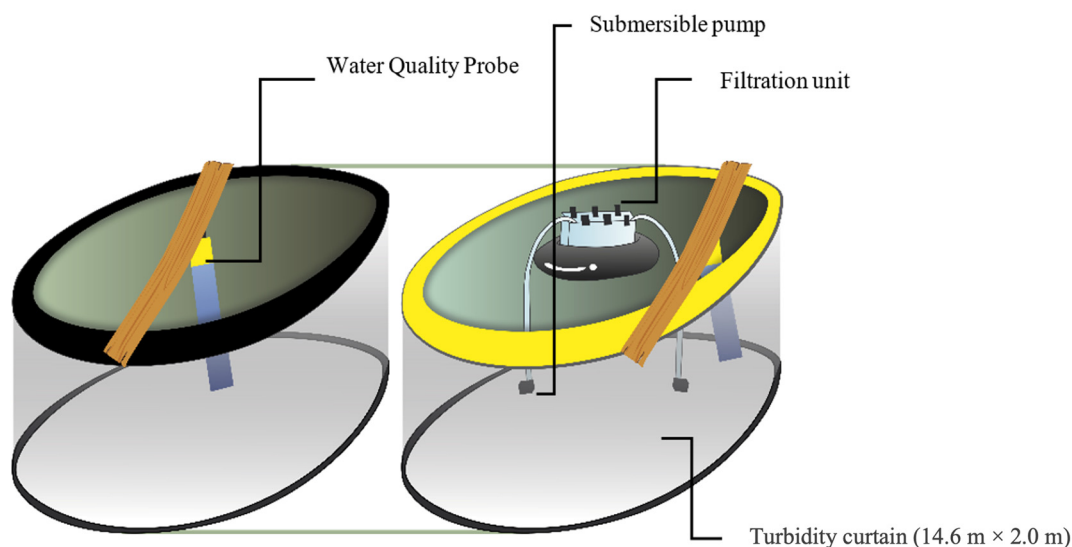


Figure 3. Schematic 3D view of the experiment enclosed areas. The control area is on the left and the filter is on the right.

In summer 2019, the two enclosed circular areas inside the lake, contained with floating turbidity curtains ($14.6 \text{ m} \times 1.2 \text{ m}$) ($L \times W$), which had approximately a diameter of 1.54 m each. In summer 2020, this diameter was increased to 2.60 m (Figure 4). If a cylindrical volume is considered (height of 1 m), the water volume to be remediated was approximately 7.45 m^3 and 21.23 m^3 for the first and second years, respectively. In both summers, one enclosed area was used to deploy the filtration unit and the other as a control. The location inside the lake was similar for both years, to have comparable results (represented by St. D in Figure 1). As shown in Figure 4, the location was chosen due to the possible harmful plankton accumulation in this area and easy access for sampling and maintenance.

2.3. Filter Media

In this filtration experiment, a combination of non-woven and woven geotextiles was used in the 2019 summer (TE-GTT170, TE-GMW35 and CM) and only custom-made woven geotextiles were employed in the 2020 summer (TE-GMW70, TE-GMW35). They were developed and received from Titan Environmental Containment Ltd., Ile des Chênes, MB, Canada. In Table 1, the geotextile physical characteristics are presented (based on the datasheets obtained from the company).



Figure 4. In-situ deployment for the control enclosed area in the two-summer experiment.

Table 1. Non-woven, woven geotextiles and mesh characteristics used in this study.

Filters	Material	AOS ^b (μm)	Flow Rate (L/m ² /min)	Permittivity (s ^{−1})	Mass Unit (g/m ²)
Commercial Mesh (CM)	PP ^a	900–450		1.62	1.80
TE-GMW70	PP ^a	658	2973	0.98	180
TE-GMW35	PP ^a	425	2039	0.70	
TE-GTT170	PP ^a	350	4800		350

Notes: ^a PP: Polypropylene; ^b AOS: Apparent Opening Size.

The TE-GTT170 is a nonwoven, white geotextile filter made of 100% virgin, UV-resistant, and thermally bonded polypropylene (PP) fibers with a 350 μm apparent opening size (AOS). The TE-GMW70 is a black woven geotextile, a multifilament, high-tenacity polypropylene fabric with UV resistance and AOS of 658 μm. The TE-GMW35 is a gray woven geotextile from the same material with an AOS of 425 μm. Those geotextiles were highly flexible and excellent for use as a filter. Lastly, the CM composed of PP was only employed in the 2019 summer experiment as a layer for removing larger suspended materials that can affect the geotextile filtration performance.

Precut 30 cm square layers were combined for experiments and placed on the floating filtration unit. For the 2019 summer, the filter selection and combination were based on the previous on-site experiment during 2017–2018 and the particle size distribution in the contained filter area. Experiments in 2017–2018 [34] were based on employing a filtration unit to filter around 300 L in batch experiments (i.e., beside the lake) and only using the larger AOS sizes used in this experiment, to determine which ones had better attenuation of suspended solids of lake water. The combination proposed was one layer of the CM, and 4–5 layers of TE-GMW35 with the addition of one TE-GTT170 when needed. In contrast, the defined combination in the second year was always 1–3 layers of the TE-GMW70, and 5–6 layers of TE-GMW35, with the number of layers defined based on the first-year study results and following the particle size in the enclosed filtration area. In the second year, the TE-GMW70 was used in the plastic tray as a prefiltration layer instead of CM. Clogged layers were entirely changed every week or when clogged, whichever occurred first. Additionally, these filter combinations from six to nine layers were used throughout the entire experiment. Figure 5 presents the woven geotextiles before the filtration process as well as a scheme of the combination used for each year (Figure 5f).

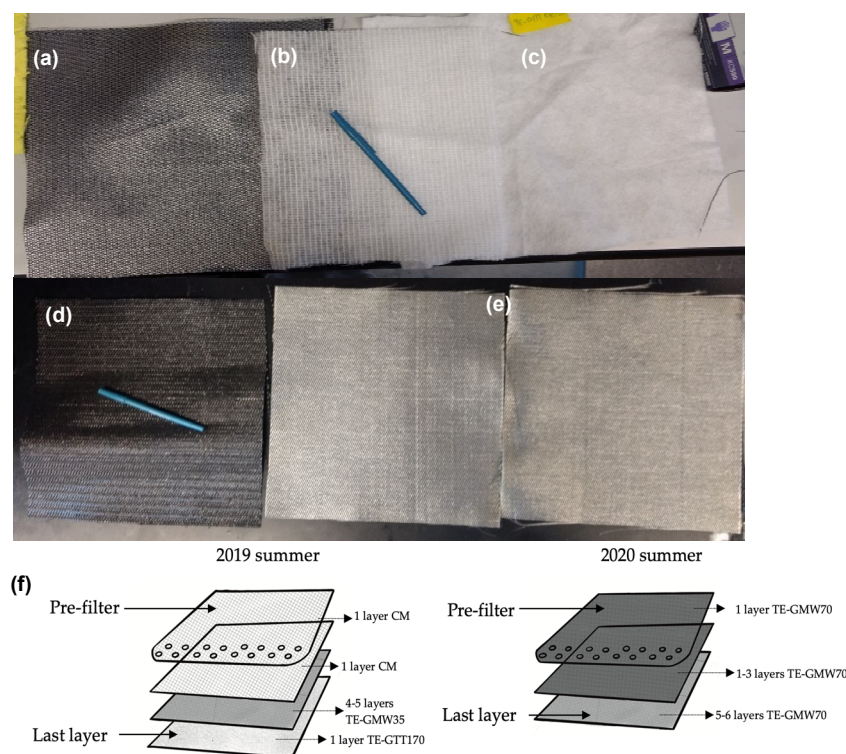


Figure 5. Geotextiles and mesh used in the experiment: (a) woven geotextile TE-GMW35—AOS: 425 µm (b) CM and (c) non-woven geotextile TE-GTT170—AOS: 350 µm before the filtration process (b) woven geotextiles used in the deployment: (d) TE-GMW70—AOS: 700 µm and (e) TE-GMW35—AOS: 425 µm before the filtration process (f) Scheme representing the number and order of geotextile layers used in the deployments.

2.4. Field Sampling and Experiment Sampling

Field sampling was performed throughout the entire lake at the six selected stations, presented in Figure 1 (St. S, St. 1, St. 4, St. 7, St. 8 and St. 9) over the 2019 and 2020 summer/fall to access the water quality of this shallow eutrophic lake water. In addition, during the filtration experiment deployment, over two consecutive summers, water samples were collected from each contained area every 2–3 days. Water samples in this project were collected in 50 mL sterilized polypropylene test tubes (chemical analysis) and previously cleaned 1 L high-density polyethylene (HDPE) amber bottles (physical analysis). Both were stored at 4 °C in the dark before any physical-chemical analysis and they were performed within 48 h.

2.5. Water Quality Analysis

Water samples were analyzed for the following parameters in both summer deployments: particle size analysis (PSA), total suspended solids (TSS), total phosphorus (TP), total nitrogen (TN), chemical oxygen demand (COD), pH, dissolved oxygen (DO), temperature (Temp.), turbidity, chlorophyll a (Chl. a) and blue-green algae-phyococyanin (BGA-PC).

Test kits from Hach Chemicals were used for accessing TP (Method 10209—SM 4500-PE—Ascorbic Acid Method), TN (TNT 826, Method 10208, persulfate digestion) and COD (TNT 820, Method 10221, reactor digestion method). For those parameters analyses water samples were first acid digested with its proper detailed method on a Hach DRB 200 heating block and after cooling down measured in a Hach DR 2800 UV-Vis spectrophotometer.

For measurements of pH, dissolved oxygen (DO), temperature (Temp.), turbidity, total dissolved solids (TDS), chlorophyll-a (Chl. a) and blue-green algae-phyococyanin (BGA-PC) during the whole experiment two YSI-EXO²™ multiparameter probes were deployed in

each contained area for hourly measurements. Probes were checked every week for data backup, battery life, and sensor performance and calibration.

To evaluate the concentration of the suspended particles in the lake water, APHA 2540 D method was used. Additionally, the particle size analysis (PSA) was measured using a laser diffraction particle analyzer (LA-960 Horiba laser particle size analyzer) for lake water samples.

2.6. Data Analysis

All study variables were analyzed for descriptive statistics including means, medians, variances, maxima, minima, standard deviations, standard errors and confidence intervals. After, verifying the existence of any outliers each variable was subsequently assessed. Data are represented as the means \pm confidence interval in the text.

To corroborate if there were statistically significant differences between water quality variables with the filter presence and absence in the lake-enclosed areas, the parametric test Student's mean *t*-test ($p < 0.05$) was used for normally distributed variables and the equivalent paired nonparametric test: Wilcoxon matched-pairs signed-ranks test ($p < 0.05$) for not normally distributed variables. While the Student's *t*-test has the null hypothesis: water quality variable means with the presence and absence of the filter are statistically equal to the Wilcoxon matched-pairs signed-ranks test ($p < 0.05$). It has a null hypothesis if the water quality variable medians with the presence and absence of the filter are equal.

In the first year as requirements for the T-student parametric test were violated (normality by the Shapiro-Wilk test ($p < 0.05$) and homoscedasticity by Levene's test ($p < 0.05$)), for the following water quality variables: PSA (i.e., D10, D50, D90), TP, TN, TSS, pH, DO, Temp., turbidity, Chl. a, BGA-PC from day 0 until day 69 in the enclosure experiment, on those the equivalent paired nonparametric test, Wilcoxon matched-pairs signed-ranks test, were employed. In contrast, the T-student parametric test was applied for the variable COD, which had normality and homoscedasticity.

In the second year as requirements for the T-student parametric test were violated, for the following water quality variables: PSA (i.e., D10, D50, D90), TP, TN, TSS, pH, DO, temperature, turbidity, Chl.a, BGA-PC, COD from day 0 until day 76 in the enclosure experiment, on those the equivalent paired nonparametric test, Wilcoxon matched-pairs signed-ranks test, were employed.

Lastly, for the relationship verification between study variables, a correlation analysis was performed using Spearman's non-parametric test ($p < 0.05$). For this specific data representation, a heat map was used.

3. Results

3.1. Lake Caron Overall Water Quality over Two Summers

Lake Caron is a mesoeutrophic lake in the middle range for phosphorus levels (20–30 $\mu\text{g/L}$) following MELCC's (2018) report [39] going towards the high range (i.e., eutrophic classification) in the near future. The phosphorus concentration in this lake is around $26 \pm 1.6 \mu\text{g/L}$ in the first year and $28.8 \pm 2.2 \mu\text{g/L}$ in the second. The maximum peak was 33 $\mu\text{g/L}$ in this lake water. No strong variation was observed between stations analysed for both years and overall results of the two consecutive summer samplings are presented in Table 2.

The turbidity in this lake, which is around 5.82 ± 3.37 FNU, is composed of particles with sizes of 50% (D50) and 90% (D90) suspended solids (SS) under $63.74 \pm 6.92 \mu\text{m}$ and $154.16 \pm 12.45 \mu\text{m}$. Even though turbidity decreased when compared with the first year (i.e., 3.24 ± 1.35 FNU), particle sizes remained like the ones previously found. TN concentrations are under Quebec guidelines (i.e., MDDEP [40]) for protecting aquatic life, which is 1.0 mg/L. Concentrations of heavy metals in the lake water (dissolved) and surface sediments are below the norm set for the protection of freshwater aquatic organisms in Quebec and Canada (not published).

Table 2. Lake Caron water quality during the two summers deployments.

Parameters	Summer 2019 ^a	Summer 2020 ^b
TP (µg/L)	26.0 ± 1.6	28.8 ± 2.2
COD (mg/L)	23.6 ± 0.2	24.0 ± 5.5
TN (mg/L)	0.81 ± 0.09	1.0 ± 0.05
TSS (mg/L)	3.5 ± 0.5	3.2 ± 1.4
D50 (µm)	63.74 ± 6.92	54.67 ± 8.63
D90 (µm)	154.16 ± 12.45	160.08 ± 18.00
YSI-EXO₂ Probe data	Summer 2019 ^c	Summer 2020 ^d
Temp (°C)	19.7 ± 0.42	18.2 ± 0.20
Conductivity (µS/cm)	23.0 ± 0.67	20.3 ± 0.11
TDS (mg/L)	14.8 ± 0.43	13.1 ± 0.04
DO (mg/L)	10.2 ± 0.04	8.37 ± 0.03
pH	6.8 ± 0.02	6.5 ± 0.01
Turbidity (FNU)	5.82 ± 3.37	3.24 ± 1.35
Chlorophyll-a (µg/L)	7.32 ± 0.56	5.82 ± 0.86
BGA-PC (µg/L)	0.51 ± 0.01	0.45 ± 0.01

Notes: ^a Average of 7 samplings of 6 lake stations; ^b Average of 4 samplings of 6 lake stations; ^c Average of 3 samplings of 6 lake stations ^d Average of 3 samplings of 6 lake stations.

Related to organic matter, the chemical oxygen demand (COD) of this lake, was mainly assumed to be in its dissolved form and did not present any significant variation in the lacustrine system remaining around 23.6 ± 0.2 mg/L and 24.0 ± 5.5 mg/L in 2019 and 2020 summers, respectively. This lake water is also well oxygenated with DO values reaching 10.2 ± 0.04 mg/L in 2019 and 8.37 ± 0.03 in 2020. The pH was near neutral in both summers and temperature was around 19.7 ± 0.42 °C and 18.2 ± 0.20 °C in the summers of 2019 and 2020, respectively. Those parameters when associated with the available nutrients are the possible requirements for increased primary productivity in this lake.

Lake water colour (i.e., which is a light tea-like colour) remained unchanged for both deployments, mainly due to previous algae blooms and some plant/tree decomposition which was not properly removed when the lake was enlarged. When phytoplankton is taken into consideration, chlorophyll-a concentration on the lake was around 7.32 ± 0.56 µg/L and 5.82 ± 0.86 µg/L, on 2019 summer and 2020 summer, respectively. Those values are mainly caused by disperse filamentous chlorophytes and possible cyanobacteria present in the whole lake throughout the hot weather. This is also one of the causes of constant replenishment of organic matter from algae decomposition processes which occur within the lake.

BGA-PC pigment associated with cyanobacteria organisms was around 0.51 ± 0.01 µg/L and 0.45 ± 0.01 µg/L in the 2019 and 2020 experiments, respectively. This indicates the presence of some cyanobacteria developing in this lake throughout the years, but due to their dispersion in the studied years no difference between stations was noticed. Additionally, lake water salinity on this lake is low as indicated by the conductivity of 23.0 ± 0.67 µS/cm and total dissolved solids (TDS) of 14.8 ± 0.43 mg/L (2019 summer) and 20.3 ± 0.11 µS/cm and 13.1 ± 0.04 mg/L in the 2020 summer.

3.1.1. Summer 2019 Deployment

In the 2019 summer, this in-situ experiment filtered approximately 7.45 m³ of lake water continuously within the enclosed area for 69 days from 14 August to 22 October of 2019, shortly after the start of the summer until the mid-fall season. The system ran smoothly without any interruption during the proposed timeframe even though the project is located inside a natural system. A summary of the physico-chemical measurements of water obtained on this year is presented in Table S1 in supplementary data.

The operation of the experimental system on a daily basis shows the adaptability of the filtration process and geotextile membranes to filter lake water in long-term projects. This was achieved by acclimating quickly to the water quality changes preventing any increase in primary productivity. In lakes, nutrients can be constantly replenished into

the overlying water from bottom sediments by the concentration gradient and sediment resuspension [34,41]. Even with those mechanisms, the system was able to maintain its removal rate throughout the whole deployment. In the control-enclosed area, visible cyanobacteria colony accumulation of possible *Woronichinia naegeliana* sp. and filamentous chlorophytes occurred as can be seen in Figure 6, which was suppressed in the filtration area. Those are the cyanobacterial predominant species existing in this lake [34].



Figure 6. Reported visible phytoplankton accumulation in the control enclosed area in 2019 summer.

With approximately 7–8 days of filtering before changing the layers, the previously mentioned combination of 1–2 layers of the CM, and 4–5 layers of TE-GMW35 with the addition of one TE-GTT170 when necessary was used. The entire deployment used 67 filter layers of TE-GMW35, 8 layers of TE-GTT 170 and 14 CM, totalling approximately 6.03 m², 0.72 m² and 1.26 m² for each AOS, respectively. The in-situ experimental cost related to only geotextile membranes (i.e., not including the CM) was \$5.05 for treating 7.45 m³ of lake water. Figure 7 presents one set of used geotextile filters after one week of lake water filtration throughout the experiments. Cake layer formation was observed on the geotextile top layer due to initial ripening that happened approximately two hours after changing the filters. The layer formed by particle accumulation decreases the AOS on those geotextiles, permitted the filtration mechanism to be employed not only by straining filtration but also by depth filtration.



Figure 7. Woven geotextiles after one week of the filtration process for AOS order: (a) CM layer (b) TE-GMW35 first layer (c) TE-GMW35 s layer (d) TE-GMW35 third layer.

3.1.2. Summer 2020 Deployment

In the 2020 summer, the in-situ experiment was deployed from 23 June 2020 to 7 October 2020, for a total of 76 days. This experiment had one more week than the first-year study but still was during the summer and fall seasons. The system operated without any major concerns, continuously removing suspended particles and their associated particulate phosphorus. The deployment followed by daily operation, of the proposed

remediation, has shown the system's possibility to maintain a continuous removal rate for a second-year long-term project, in a larger enclosed area of 2.60 m when compared with the 1.54 m diameter of the first year. A summary of the physico-chemical measurements of water obtained on this year is presented in Table S2 in supplementary data.

Using only woven geotextile membranes with larger AOS, the filter run was maintained 7 days before requiring a geomembrane combination change. The combination of layers consumed approximately 50 square filter layers of TE-GMW70 and 132 filter layers of TE-GMW35. Approximately 3.96 m² and 11.88 m² for each AOS were used. This results in a cost of \$29.70 when related only to TE-GMW35 for remediation of approximately 21.2 m³ of lake water. Additionally, the floating filtration system was able to support a strong particle and associated parameter removal rate, during the whole experiment. Cake superficial development, on the geotextile, is shown in Figure 8, after one-week filtration. This filter ripening ensured AOS reduction by not only filtering the water from particle sizes (i.e., straining) but by forming a filter cake (i.e., depth filtration).

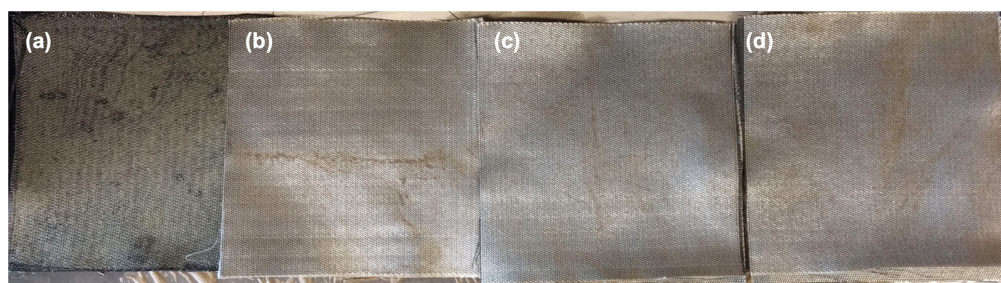


Figure 8. Woven geotextiles after the filtration process: (a) TE-GMW70—AOS: 700 µm, (b) TE-GMW35 s layer—AOS: 425 µm, (c) TE-GMW35 third layer—AOS: 425 µm and (d) TE-GMW35 fourth layer—AOS: 425 µm.

Visible cyanobacteria formation was observed for possible *W. naegeliana* sp., as well as chlorophytes which accumulated at the shore due to wind action during the morning as presented in Figure 9. Those organisms (i.e., *W. naegeliana* sp.) have gas vesicles, providing mechanisms to move up and down in the water column, which increases access to nutrients and other growth factors. No visible phytoplankton formation was observed in both enclosed areas.



Figure 9. Floating phytoplankton in Lake Caron in the 2020 summer study.

3.2. Total Suspended Solids and Turbidity Attenuation

In the deployment, there was a constant and representative removal of total suspended solids (TSS) as the filter unit quickly adapted to changes in this natural system. Statistically significant TSS removal ($p < 0.01$) was observed in this project with an average value of 53% on the 2019 summer. After the fourth day of filtration the removal trend was always better in the experiment than the control system as shown in Figure 10. By the end of the experiment, the control enclosed area had an average TSS concentration of 3.69 ± 0.45 mg/L and the filter enclosed area had 1.72 ± 0.51 mg/L.

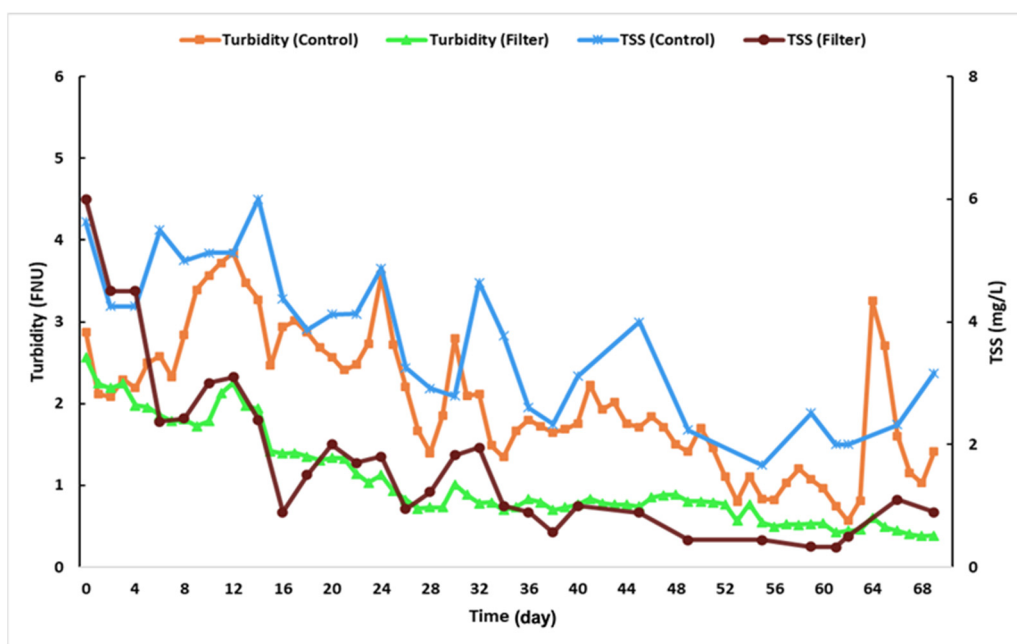


Figure 10. Turbidity (FNU) and total suspended solids concentrations (mg/L) for the 2019 summer in situ experiment.

Similar to the TSS removal in the filtration enclosed area, turbidity reduction is presented in Figure 10. The floating filtration unit was able to maintain an average removal of 49%, statistically significant ($p < 0.01$) decreasing, even more when there was low turbidity in the lake. There was also a strong correlation between those two variables ($R^2 = 0.833$, p -value < 0.01). Instead, in the control area, a tendency of constant increases in the SS concentration and turbidity occurred. This was possibly caused by the reported visible algae/cyanobacteria colony accumulation in this area, which only decreased when the water temperature started to drop. However, in the filtration-enclosed area, values went below 1 FNU shortly after the middle of the experiment was reached. This showed the geotextile membrane filtration effectiveness in this lake water. The average values present in each enclosed area were 2.02 ± 0.05 FNU in the control area and 1.04 ± 0.03 FNU in the filter area.

In the 2020 summer study, a larger enclosed area was used with a similar flow rate, filtration unit and geotextile area. Additionally, larger AOS woven geotextile filters were employed. Statistically significant TSS removal is shown in Figure 11 which was an average of 37% ($p < 0.01$). This has enabled water TSS concentration to be below 3.0 mg/L after the tenth day until the end of the test. By the end of the experiment, the control enclosed area has a TSS concentration average value of 4.23 ± 0.32 mg/L and the filter enclosed area had 2.67 ± 0.37 mg/L.

Average turbidity removal in the filter-enclosed area was 17%, as presented in Figure 11, which was statistically significant ($p < 0.01$). An experimental average of 2.92 ± 0.05 FNU was obtained in the control area and 2.42 ± 0.03 FNU in the filtration-enclosed area. This removal percentage was lower than in the previous study.

With the TSS and turbidity attenuation in the 2019 summer, a reduction in the particle size was also assessed in the filtration-enclosed area as statistically significant. While in the filter-enclosed area average values showed 50% (D50) and 90% (D90) of TSS were $<28.40 \pm 4.87$ μm and $<77.94 \pm 10.12$ μm , the control area values were $<36.45 \pm 4.71$ μm and $<154.07 \pm 9.33$ μm respectively. There was also a statistically significant positive correlation between D90 size reduction and turbidity in the filtration-enclosed area ($R^2 = 0.8543$, p -value < 0.01). The reduction showed that particles between these D90 (i.e., 77.94 ± 10.12 μm $>$ D90 $>154.07 \pm 9.33$ μm) were the ones addressed by the geomembranes and possibly the ones with particulate contaminants and nutrients associated with them, as further evaluated. In the 2020 summer, the

control-enclosed area particle size average showed 50% (D50) and 90% (D90) of TSS as presented. They were $<52.85 \pm 7.47 \mu\text{m}$ and $<158.60 \pm 6.64 \mu\text{m}$ and $<54.57 \pm 6.26 \mu\text{m}$ and $<142.36 \pm 9.25 \mu\text{m}$, in the control and filter areas, respectively.

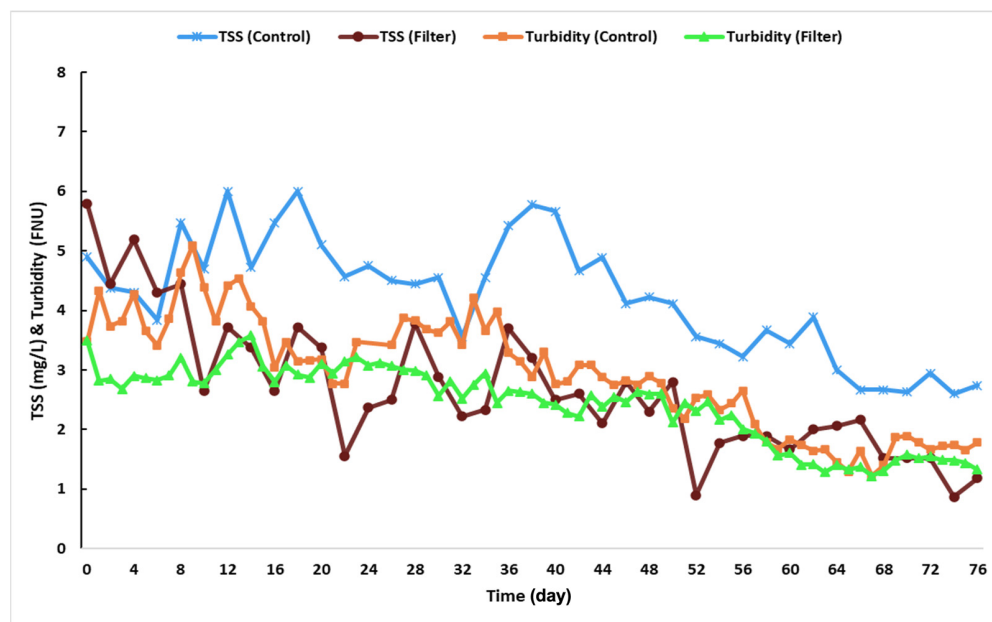


Figure 11. Turbidity (FNU) and total suspended solids concentrations (mg/L) for the 2020 summer in situ experiment.

The water temperature in 2019 summer was of $16.3 \pm 0.27 \text{ }^{\circ}\text{C}$ with the maximum water temperature in the experiment reached on its first days of $21.8 \text{ }^{\circ}\text{C}$. In the 2020 summer, the average value of water temperature presented was $19.2 \pm 0.20 \text{ }^{\circ}\text{C}$, with a maximum water temperature reaching $27 \text{ }^{\circ}\text{C}$ in the first week of summer.

3.3. Nutrient and Organic Matter Removal

The removal and size decrease in suspended particles affected the nutrient concentration in the enclosed filtration area in the 2019 summer study. Most precisely particulate phosphorus removal in the system was continually achieved by recirculating water on the floating filtration unit as presented in Figure 12. A good positive correlation between turbidity and total phosphorus removal was found ($R^2 = 0.6240$, $p\text{-value} < 0.01$). The TP removal was statistically representative ($p < 0.01$) with a 22% average removal as shown in Figure 12.

In contrast, throughout the experiments, no significant statistical change in the concentrations of TN was observed, as they were mainly (>80%) in their dissolved form. Lake water was already within the Quebec-regulated guidelines for this parameter and the average value for both enclosed areas was kept below the values presented. For TN concentrations the values were 1.03 ± 0.06 and $1.08 \pm 0.06 \text{ mg/L}$, in the control and filter enclosed area, respectively, in the 2019 summer.

Removal of suspended particles and associated particulate nutrients prevents them from settling and enabling the growth of possible harmful plankton. The associated particulate nutrient such as total phosphorus in the filter-enclosed area was reduced. In the 2019 summer study, the lake water was at a eutrophic level (average concentration of $29.0 \pm 1.5 \mu\text{g/L}$) but was reduced to the limit of mesoeutrophic going towards the mesotrophic (filter-enclosed area of $22.7 \pm 1.4 \mu\text{g/L}$) which has been represented as a statistically representative average removal of 22% in Figure 12.

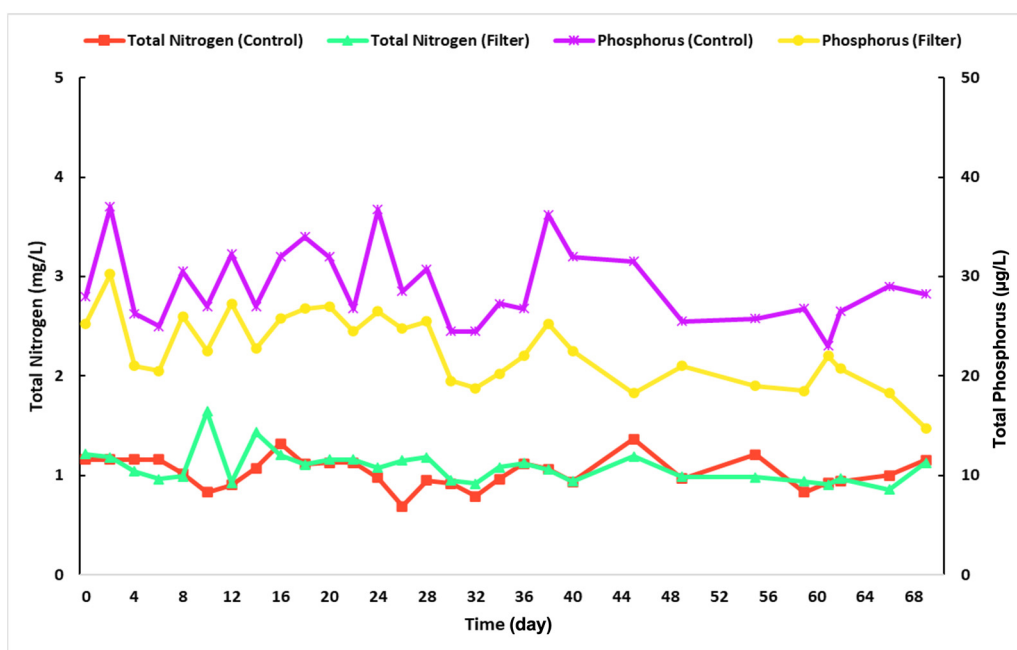


Figure 12. TP concentrations ($\mu\text{g/L}$) and TN concentrations (mg/L) for the 2019 summer in-situ experiment.

In the 2020 summer study, lake water TP removal had the same behaviour as the first-year study. A higher average level in the control enclosed area was $34.1 \pm 1.2 \mu\text{g/L}$, which is at the higher limit of the mesoeutrophic trophic level. However, in the filter area, the average was $27.8 \pm 0.6 \mu\text{g/L}$, as shown in Figure 13. The TP removal in this study was statistically representative ($p < 0.01$) with a 19% average removal. No correlation between turbidity and TP removal as well as TSS and TP was found. This could be explained as a significant number of particles were not reduced and removed in the system for TP reduction to occur. The average values of TN were $1.57 \pm 0.09 \text{ mg/L}$ and $1.54 \pm 0.10 \text{ mg/L}$ for the control and the filter area.

3.4. Algae/Cyanobacteria Removal

The average values for chlorophyll-a were $7.30 \pm 0.09 \mu\text{g/L}$ for the enclosed control area and $3.13 \pm 0.08 \mu\text{g/L}$ for the filter area, which represents a statistically significant removal of 57% ($p < 0.01$). As visible algae/cyanobacteria formation was not observed in the filter area, similar removal trends for TSS, turbidity and particulate TP were obtained. All of them were found to be statistically correlated with chlorophyll-a which explained the absence of primary productivity.

BGA removal, which was 56% ($p < 0.01$) in the system. Cyanobacteria development was observed in the control but not in the filter area, as shown in Figure 14. The average values for BGA were $0.51 \pm 0.01 \mu\text{g/L}$ for the control enclosed area and $0.23 \pm 0.01 \mu\text{g/L}$ for the filter area.

In the 2020 summer, chlorophyll-a in the filter area was always lower than the control area with average values for chlorophyll-a of $5.66 \pm 0.06 \mu\text{g/L}$ and $3.85 \pm 0.05 \mu\text{g/L}$ for the filter area, which represents a statistically significant removal of 32% ($p < 0.01$) (Figure 15). This was less than the first-year study that showed 57% chlorophyll-a removal. The filtration system was able to suppress primary productivity to some level in the experiment. Total suspended solids (TSS) ($R^2 = 0.61$, p -value < 0.01) and turbidity ($R^2 = 0.55$, p -value < 0.01) were found to be statistically correlated with chlorophyll-a meaning that the suspended solids are mainly photosynthetic matter such as algae, etc.

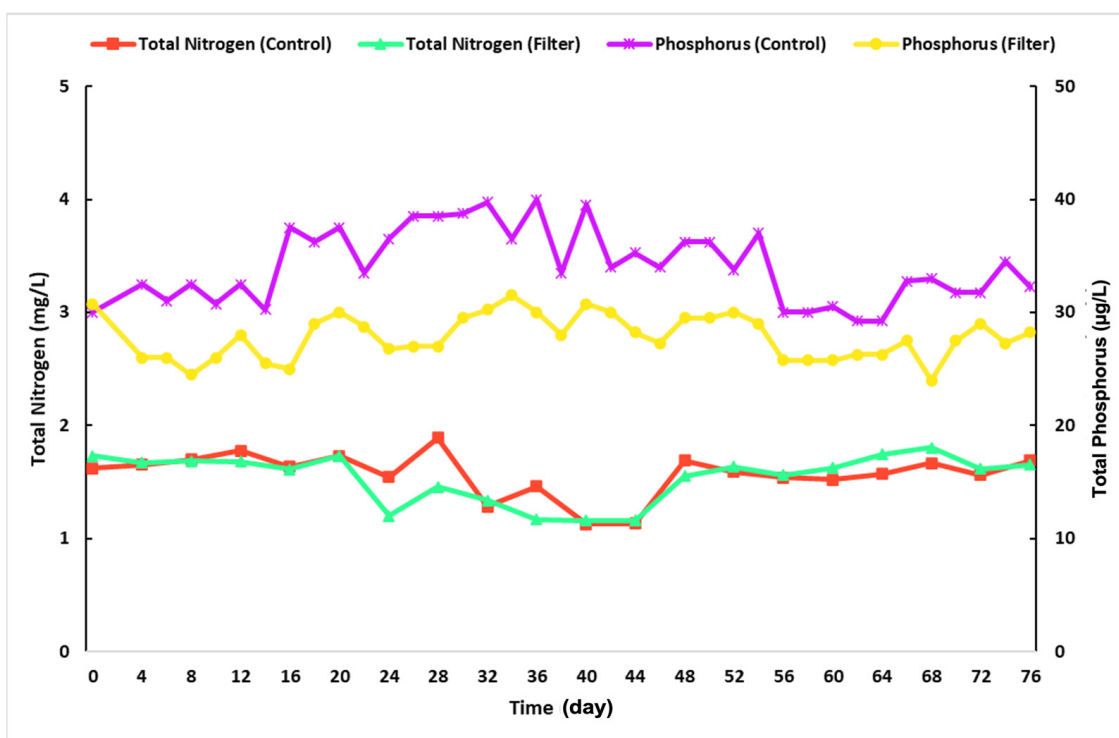


Figure 13. TP concentrations ($\mu\text{g/L}$) and TN concentrations (mg/L) for the 2020 summer in situ experiment.

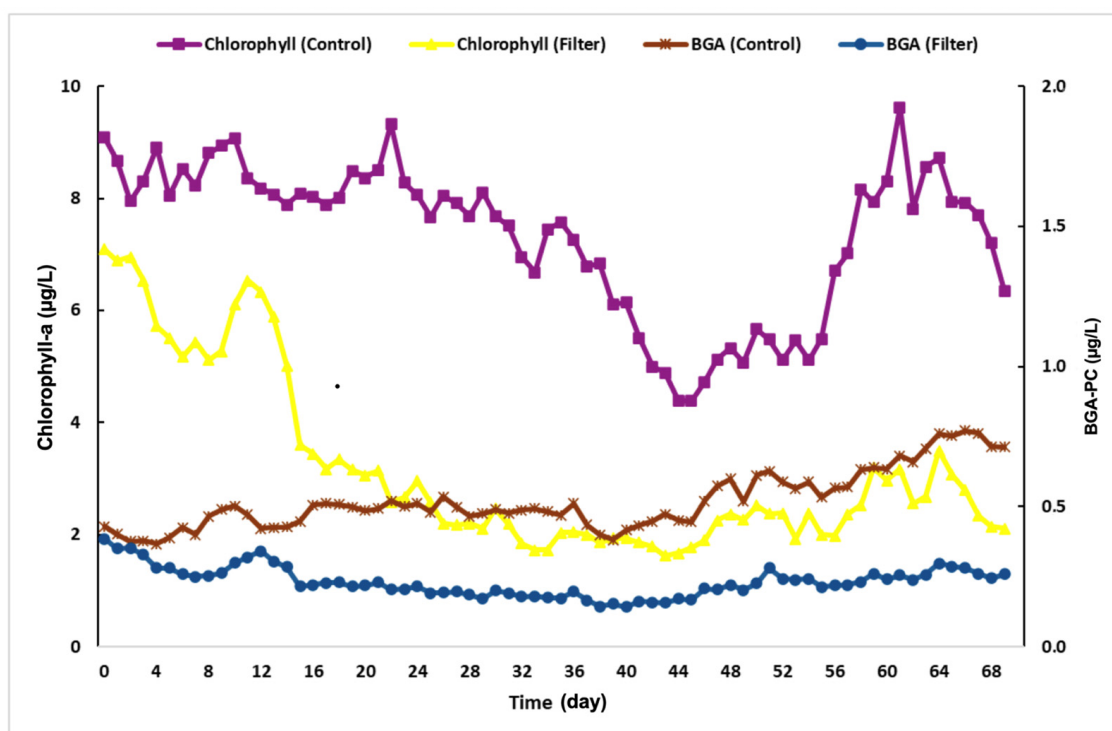


Figure 14. Chlorophyll-a ($\mu\text{g/L}$) and BGA-PC concentrations ($\mu\text{g/L}$) for the 2019 summer in-situ experiment.

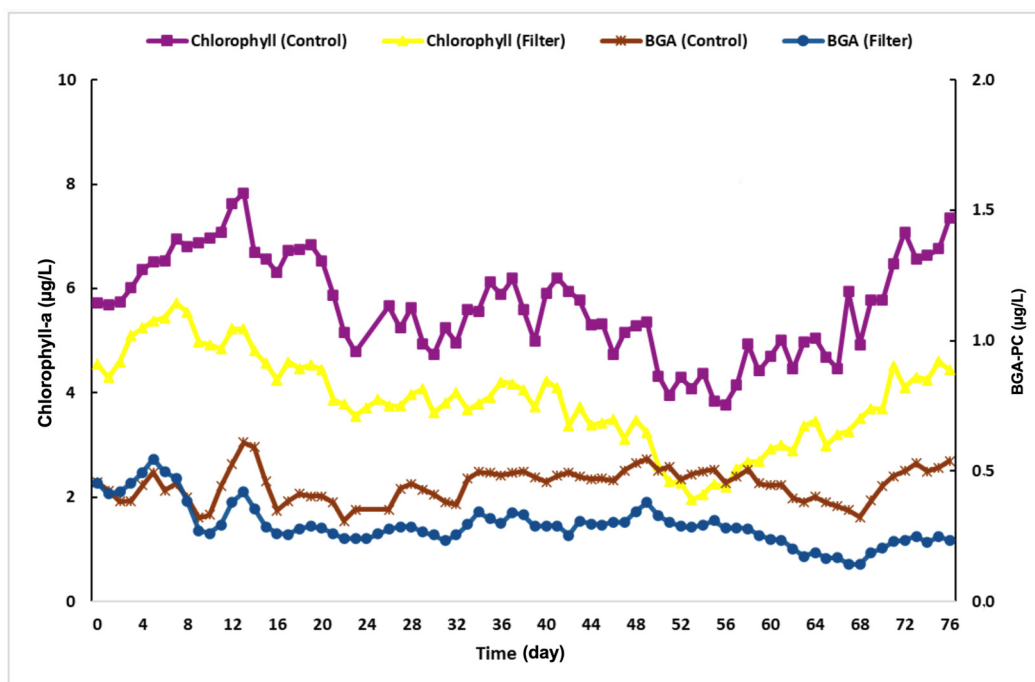


Figure 15. Chlorophyll-a ($\mu\text{g/L}$) and BGA-PC concentrations ($\mu\text{g/L}$) for the 2020 summer in situ experiment.

The BGA parameter in the filter area was always lower than the control area as well. As commented, cyanobacteria formation was observed in this lake water but at low densities. This has been shown as the average values for BGA, which were $0.45 \pm 0.004 \mu\text{g/L}$ for the control-enclosed area and $0.29 \pm 0.004 \mu\text{g/L}$ for the filter area, which represents a statistically significant removal of 35% ($p < 0.01$) which was less than the first-year study. This could be considered as an indication that this floating filtration unit is a potentially environmentally harmless, flexible and efficient remediation method in removing algae/cyanobacteria development for an entire season.

3.5. Experimental Correlations

The correlation analysis using Spearman's non-parametric test ($p < 0.05$) was chosen as a way to represent any monotonic relationship between the two variables in the proposed treatment (i.e., filter-enclosed area). In other words, the matrix presented variables that change with the same compartment but not necessarily at a constant linear rate. Heatmap representation for the two summers deployment is presented on Figures S1 and S2 in the supplementary data for 2019 and 2020, respectively. Not statically significantly correlations ($p > 0.01$) are crossed out.

In the 2019 summer, turbidity and TSS present strong correlations with important variables of the filtration process for particle removal: D90, D50, TP, COD and chlorophyll-a. In other words, all variables that could characterize particles in some way present a good and excellent correlation between them. This validates that the in-situ geotextile process applied in which the removal of particles is responsible for the absence of algae/cyanobacteria, reduction in phosphorus levels and decrease in particle sizes.

Well-known correlations in lake water were also presented in this study such as conductivity and DO, conductivity and temperature, and temperature and DO. Additionally, the water temperature was strongly correlated with SS and turbidity behaviour in this process. When water temperature rises, this will cause a reduction in the DO concentration.

Negative relations were also presented in the system; one of the most representative was DO and turbidity and TSS and DO. To better explain, as there are more particles in the water, DO decreased as the dissolved oxygen was used in other processes in the natural

system. The inverse was also true in this process when the removal of these particles, the main objective of the applied process, was to increase the dissolved oxygen content.

In the 2020 summer, the same performance was as the previous one, where variables that can characterize particles presented a strong correlation with turbidity and TSS removal. These variables were D90, BGA, COD and chlorophyll-a. This confirms that this in-situ geotextile process can be applied in a large, enclosed area for a long-time project to remediate lake water.

Strong negative correlations were found with DO and variables such as turbidity, water temperature, COD, TSS and conductivity. This can be explained by the quantity of DO dissolving in the water is affected by the water temperature. Additionally, DO can affect the growth of algae and water cloudiness.

4. Discussion

Even though the project only affects the suspended solids (SS) content in the water area defined the silt curtain, there is also possible interaction of water and sediment as well within the curtain, replenishing the nutrients into the overlying water. In contrast, the floating filtration unit was able to quickly respond and maintain the treatment of the lake water. In other words, it was hypothesized that the removal of suspended particles should be the most important, as it is the main application of any filtration system for both deployments. Additionally, by removing those SS particles present in the lake due to external or internal loads, there was the prevention of a possible future settling which can directly affect the nutrient and contaminants within the lake sediment.

The water that was near the limit of being considered eutrophic water was reduced to the limit of mesoeutrophic going towards the mesotrophic level for both summers using geotextile filtration. By regulating primary production, the limiting nutrient for this lake was considered phosphorus, which was reduced by this geotextile membrane filtration. On average the removal was 22% and 19% in the 2019 and 2020 summers, respectively.

Related to SS, there was an observed trend as the control area was always higher than the removal in the filtration-enclosed area. This has shown that the floating system used was able to quickly respond and remediate the water despite suspended solids and nutrient replacement due to sediment resuspension, and watershed runoff. TSS and turbidity strong correlation were captured ($R^2 = 0.833$, p -value < 0.01) in the filter-enclosed area in the first-year study. Instead, in the control area, a tendency of constant increases in the SS concentration and turbidity was captured. This was possibly caused by the reported visible algae/cyanobacteria colony accumulation in this area, which decreased when the water temperature started to drop and aquatic organisms started to decrease, degrade and settle on the lake sediment. In the second year, there was a statistically significant positive correlation between D90 size reduction and turbidity in the filtration enclosed area ($R^2 = 0.56$, p -value < 0.01) and D90 and BGA ($R^2 = 0.64$, p -value < 0.01). An explanation of this correlation can be that those particles were in most cases, photosynthetic organisms such as cyanobacteria, which were captured by the filter's layers.

By this second-year study, by increasing the filtration area but using the same flow rate and the same geotextile floating unit with woven layers, the same removal was obtained. Continuously remediating the lake water in the enclosed filter area, average removal was reduced in the 2020 year when compared with the 2019 summer study. As there was less water to be filtered in the first year and the commercial mesh (CM) membrane (i.e., used as pre-filtration for this project) presents fiber-like comportment in capturing algae/cyanobacteria, which has improved the filtration removal of suspended solids by employing the depth filtration mechanism. A large, enclosed area will require the scale-up on the filtration unit, which will require a higher filter area as well as a higher flow rate pump. This requirement would be used to produce a further methodology for the potential full-scale implementation of this remediation technique. Also, for future applications of this eco-remediation in other water types, SS sizes and compositions present in the water (i.e., sizes of contaminated SS and sizes of harmful algae/cyanobacteria) can be focused on.

Removing particles by the geotextiles decreased the overall particle size and addressed particulate nutrients to prevent them from settling and possibly being available in the water column for easy uptake by harmful plankton. The floating filtration in-situ unit was able to maintain a nutrient removal trend, even though it has been constantly replenished within the natural system. It suppressed any algae/cyanobacteria development. This is the final corroboration of this in-situ geotextile filtration as a flexible, potentially economically efficient, reactive and environmentally safe remediation in preventing algae/cyanobacteria formation for an entire season.

With this understanding this remediation is not only applicable for shallow lakes (average depth < 2 m) but also ponds, river sections, coastal regions and bays that have similar issues. As the filtration unit is easy to operate and maintain, the deployed system did not need a highly trained technician, which is a plus. Additionally, possible pre-filtration (with higher pore sizes) for any large debris removal is recommended before the application of the water in the geotextiles, to prevent rapid clogging.

Operational costs of this method are associated with electricity for continuous pumping, which is about 68% of the total value. It is recommended for any future applications to use alternative energy sources such as renewable ones (i.e., solar or wind energy), depending on the installed location.

Further investigations and development possibly addressed in near future will be the following: an increased enclosed area for the proposed treatment, application of other geotextile AOS sizes, geotextile layers reuse after high-pressure washing and natural drying, and uptake of dissolved organic matter by microorganisms using ceramsite (i.e., porous clay particles produced by pelletizing and sintering) as support media combined with filtration. Additionally, consideration will be given to the lake water dissolved organic matter characterization, understanding internal release mechanics within the lake water lastly, related to the captured sediment, in-situ dewatering of the SS captured by evaporation followed by assessment for direct application or final disposal.

5. Conclusions

The in-situ experiment showed that geotextile filtration is an effective, environmentally safe, and economic method for which SS and particulate nutrients can be reduced and algae and cyanobacteria development suppressed in two entire recreational seasons in lake water. The geotextile filter combination used allowed TP, TSS, and turbidity removal and reduced particle sizes directly affecting the chlorophyll-a and BGA concentrations (i.e., primary productivity) in the system. Even though with constant nutrient replenishment into the overlying water, removal trends were maintained showing the adaptability of the applied methodology. Preventing particles from settling which could include harmful plankton, is strongly statistically positively correlated with TSS and turbidity, variables that represent particles in the system (total phosphorus (TP), turbidity, chlorophyll-a). The lake water was decreased to the limit of mesoeutrophic going towards the mesotrophic state with this filtration process. For future work, attention will be made to the clogged geotextile filter reuse, dissolved COD uptake in the lake water and captured sediment dewatering and final disposal. Possible larger in-situ filtration pilot experiments will be assessed in this project.

Supplementary Materials: The following supporting information can be downloaded at: <https://www.mdpi.com/article/10.3390/w15030441/s1>, Figure S1: Heat map representation of the Spearman correlation matrix on all variables for the summer 2019 deployment, not statically significantly correlation ($p > 0.01$) is crossed out; Figure S2: Heat map representation of the Spearman correlation matrix on all variables for the summer 2020 deployment, not statically significantly correlation ($p > 0.01$) is crossed out; Table S1. Lake Caron physico-chemical measurements and descriptive statistics for summer 2019 deployment; Table S2. Lake Caron physico-chemical measurements and descriptive statistics for summer 2020 deployment.

Author Contributions: Conceptualization, A.C.P.; methodology, A.C.P. and C.N.M.; investigation, A.C.P., D.P.V. and S.B.; writing—original draft preparation, A.C.P.; writing—review and editing, C.N.M.; visualization, A.C.P.; supervision, C.N.M.; project administration, C.N.M.; funding acquisition, C.N.M. and S.B. All authors have read and agreed to the published version of the manuscript.

Funding: This research was funded by NSERC (ALLRP 549706-19), Concordia University and Titan Environmental Containment.

Institutional Review Board Statement: Not applicable.

Informed Consent Statement: Not applicable.

Data Availability Statement: The data for this study is available from the authors upon reasonable request.

Acknowledgments: The authors are also grateful to their industrial partner, Titan Environmental Containment Ltd., for supplying geotextiles and providing technical support for this project.

Conflicts of Interest: The authors declare no conflict of interest.

References

1. Le Moal, M.; Gascuel-Oudou, C.; Ménesguen, A.; Souchon, Y.; Étrillard, C.; Levain, A.; Moatar, F.; Pannard, A.; Souchu, P.; Lefebvre, A.; et al. Eutrophication: A new wine in an old bottle? *Sci. Total Environ.* **2019**, *651*, 1–11. [\[CrossRef\]](#) [\[PubMed\]](#)
2. Yindong, T.; Xiwen, X.; Miao, Q.; Jingjing, S.; Yiyan, Z.; Wei, Z.; Penghu, W.; Xijun, W.; Yang, Z. Lake warming intensifies the seasonal pattern of internal nutrient cycling in the eutrophic lake and potential impacts on algal blooms. *Water Res.* **2021**, *188*, 116570. [\[CrossRef\]](#) [\[PubMed\]](#)
3. Woolway, R.I.; Merchant, C.J. Worldwide alteration of lake mixing regimes in response to climate change. *Nat. Geosocial.* **2019**, *12*, 271–276. [\[CrossRef\]](#)
4. Freeman, E.C.; Creed, I.F.; Jones, B.; Bergstrom, A. Global changes may be promoting a rise in select cyanobacteria in nutrient-poor northern lakes. *Glob. Change Biol.* **2020**, *26*, 4966–4987. [\[CrossRef\]](#)
5. Burford, M.; Carey, C.; Hamilton, D.; Huisman, J.; Pearl, H.; Wood, S.; Wulff, A. Perspective: Advancing the research agenda for improving understanding of cyanobacteria in a future of global change. *Harmful Algae* **2020**, *91*, 101601. [\[CrossRef\]](#)
6. Braga, G.G.; Becker, V. Influence of water volume reduction on the phytoplankton dynamics in a semi-arid man-made lake: A comparison of two morphofunctional approaches. *An. Acad. Bras. Ciências* **2020**, *92*, 1–17. [\[CrossRef\]](#) [\[PubMed\]](#)
7. Hayden, B.; Harrod, C.; Thomas, S.M.; Eloranta, A.P.; Myllykangas, J.; Siwertsson, A.; Præbel, K.; Knudsen, R.; Amundsen, P.; Kahilainen, K.K. From clear lakes to murky waters—Tracing the functional response of high-latitude lake communities to concurrent ‘greening’ and ‘browning’. *Ecol. Lett.* **2019**, *22*, 807–816. [\[CrossRef\]](#)
8. Meyer-Jacob, C.; Michelutti, N.; Paterson, A.M.; Cumming, B.F.; Keller, W.B.; Smol, J.P. The browning and re-browning of lakes: Divergent lake-water organic carbon trends linked to acid deposition and climate change. *Sci. Rep.* **2019**, *9*, 16676. [\[CrossRef\]](#)
9. Kritzberg, E.S.; Hasselquist, E.M.; Škerlep, M.; Löfgren, S.; Olsson, O.; Stadmark, J.; Valinia, S.; Hansson, L.A.; Laudon, H. Browning of freshwaters: Consequences to ecosystem services, underlying drivers, and potential mitigation measures. *Ambio* **2019**, *49*, 375–390. [\[CrossRef\]](#)
10. Paerl, H.W.; Havens, K.E.; Xu, H.; Zhu, G.; McCarthy, M.J.; Newell, S.E.; Scott, J.T.; Hall, N.S.; Otten, T.G.; Qin, B. Mitigating eutrophication and toxic cyanobacterial blooms in large lakes: The evolution of a dual nutrient (N and P) reduction paradigm. *Hydrobiologia* **2019**, *847*, 4359–4375. [\[CrossRef\]](#)
11. Jeppesen, E.; Pierson, D.; Jennings, E. Effect of Extreme Climate Events on Lake Ecosystems. *Water* **2021**, *13*, 282. [\[CrossRef\]](#)
12. Eimers, M.C.; Liu, F.; Bontje, J. Land Use, Land Cover, and Climate Change in Southern Ontario: Implications for Nutrient Delivery to the Lower Great Lakes. In *The Handbook of Environmental Chemistry*; Springer: Cham, Switzerland, 2020; pp. 235–249. [\[CrossRef\]](#)
13. Sinha, E.; Michalak, A.M.; Balaji, V. Eutrophication will increase during the 21st century as a result of precipitation changes. *Science* **2017**, *357*, 405–408. [\[CrossRef\]](#) [\[PubMed\]](#)
14. Huo, S.; He, Z.; Ma, C.; Zhang, H.; Xi, B.; Xia, X.; Xu, Y.; Wu, F. Stricter nutrient criteria are required to mitigate the impact of climate change on harmful cyanobacterial blooms. *J. Hydrol.* **2019**, *569*, 698–704. [\[CrossRef\]](#)

15. Stockwell, J.D.; Doubek, J.P.; Adrian, R.; Anneville, O.; Carey, C.C.; Carvalho, L.; De Senerpont, L.N.D.; Dur, G.; Frassl, M.A.; Grossart, H.; et al. Storm impacts on phytoplankton community dynamics in lakes. *Glob. Change Biol.* **2020**, *26*, 2756–2784. [CrossRef] [PubMed]
16. Zhang, S.; Wang, W.; Zhang, K.; Xu, P.; Lu, Y. Phosphorus release from cyanobacterial blooms during their decline period in eutrophic Dianchi Lake, China. *Environ. Sci. Pollut. Res.* **2018**, *25*, 13579–13588. [CrossRef] [PubMed]
17. Senar, O.E.; Creed, I.F.; Trick, C.G. Lake browning may fuel phytoplankton biomass and trigger shifts in phytoplankton communities in temperate lakes. *Aquat. Sci.* **2021**, *83*, 21. [CrossRef]
18. Knoll, L.B.; Morgan, A.; Vanni, M.J.; Leach, T.H.; Williamson, T.J.; Brentrup, J.A. Quantifying pelagic phosphorus regeneration using three methods in lakes of varying productivity. *Inland Waters* **2016**, *6*, 509–522. [CrossRef]
19. Kong, M.; Chao, J.; Han, W.; Ye, C.; Li, C.H.; Tian, W. Degradation Characteristics of Phosphorus in Phytoplankton-Derived Particulate Organic Matter and Its Effects on the Growth of Phosphorus-Deficient *Microcystis aeruginosa* in Lake Taihu. *Int. J. Environ. Res. Public Health* **2019**, *16*, 2155. [CrossRef]
20. Paerl, H.W.; Havens, K.E.; Hall, N.S.; Otten, T.G.; Zhu, M.; Xu, H.; Zhu, G.; Qin, B. Mitigating a global expansion of toxic cyanobacterial blooms: Confounding effects and challenges posed by climate change. *Mar. Freshw. Res.* **2020**, *71*, 579. [CrossRef]
21. Maberly, S.C.; Pitt, J.A.; Davies, P.S.; Carvalho, L. Nitrogen and phosphorus limitation and the management of small productive lakes. *Inland Waters* **2020**, *10*, 159–172. [CrossRef]
22. Sandström, S.; Futter, M.N.; Kyllmar, K.; Bishop, K.; O'Connell, D.W.; Djodjic, F. Particulate phosphorus and suspended solids losses from small agricultural catchments: Links to stream and catchment characteristics. *Sci. Total Environ.* **2020**, *711*, 134616. [CrossRef] [PubMed]
23. Bormans, M.; Maršálek, B.; Jančula, D. Controlling internal phosphorus loading in lakes by physical methods to reduce cyanobacterial blooms: A review. *Aquat. Ecol.* **2015**, *50*, 407–422. [CrossRef]
24. Niemistö, J.; Silvonen, S.; Horppila, J. Effects of hypolimnetic aeration on the quantity and quality of settling material in a eutrophied dimictic lake. *Hydrobiologia* **2019**, *847*, 4525–4537. [CrossRef]
25. Ruuhijärvi, J.; Malinen, T.; Kuoppamäki, K.; Ala-Opas, P.; Vinni, M. Responses of food web to hypolimnetic aeration in Lake Vesijärvi. *Hydrobiologia* **2020**, *847*, 4503–4523. [CrossRef]
26. Jing, L.; Bai, S.; Li, Y.; Peng, Y.; Wu, C.; Liu, J.; Xie, Z.; Yu, G. Dredging project caused short-term positive effects on lake ecosystem health: A five-year follow-up study at the integrated lake ecosystem level. *Sci. Total Environ.* **2019**, *686*, 753–763. [CrossRef] [PubMed]
27. Spears, B.M.; Mackay, E.B.; Yasseri, S.; Gunn, I.D.; Waters, K.E.; Andrews, C.; Cole, S.; De Ville, M.; Kelly, A.; Meis, S.; et al. A meta-analysis of water quality and aquatic macrophyte responses in 18 lakes treated with lanthanum-modified bentonite (Phoslock®). *Water Res.* **2016**, *97*, 111–121. [CrossRef]
28. Waajen, G.; van Oosterhout, F.; Lüring, M. Bio-accumulation of lanthanum from lanthanum modified bentonite treatments in lake restoration. *Environ. Pollut.* **2017**, *230*, 911–918. [CrossRef]
29. Liu, B.; Liu, L.; Li, W. Effective removal of phosphorus from eutrophic water by using cement. *Environ. Res.* **2020**, *183*, 109218. [CrossRef]
30. Huser, B.J.; Egemose, S.; Harper, H.; Hupfer, M.; Jensen, H.; Pilgrim, K.M.; Reitzel, K.; Rydin, E.; Futter, M. Longevity and effectiveness of aluminum addition to reduce sediment phosphorus release and restore lake water quality. *Water Res.* **2016**, *97*, 122–132. [CrossRef]
31. Agstam-Norlin, O.; Lannergård, E.; Futter, M.; Huser, B. Optimization of aluminum treatment efficiency to control internal phosphorus loading in eutrophic lakes. *Water Res.* **2020**, *185*, 116150. [CrossRef]
32. Lüring, M.; Mackay, E.; Reitzel, K.; Spears, B.M. Editorial—A critical perspective on geo-engineering for eutrophication management in lakes. *Water Res.* **2016**, *97*, 1–10. [CrossRef]
33. Lüring, M.; Mucci, M. Mitigating eutrophication nuisance: In-lake measures are becoming inevitable in eutrophic waters in the Netherlands. *Hydrobiologia* **2020**, *847*, 4447–4467. [CrossRef]
34. Palakkeel Veetil, D.; Arriagada, E.C.; Mulligan, C.N.; Bhat, S. Filtration for improving surface water quality of a eutrophic lake. *J. Environ. Manag.* **2021**, *279*, 111766. [CrossRef] [PubMed]
35. Pereira, A.C.; Veetil, D.P.; Mulligan, C.N.; Bhat, S. On-site non-woven geotextile filtration method for remediation of lake water. In Proceedings of the 2020 CSCE Annual Conference, Saskatoon, SK, Canada, 27–30 May 2020. Available online: <https://www.titanenviro.com/wp-content/uploads/2021/02/CSCE-Paper-May-2020.pdf> (accessed on 22 December 2022).
36. Mulligan, C.N.; Davarpanah, N.; Fukue, M.; Inoue, T. Filtration of contaminated suspended solids for the treatment of surface water. *Chemosphere* **2009**, *74*, 779–786. [CrossRef] [PubMed]
37. Couture, H.M.; Goulin, B.; Gutjahr, B.; Mercier, C. *Stratégie de Protection et de Mise en Valeur des Milieux Humides sur le Territoire de la Municipalité de Sainte-Anne-des-Lacs*; Université de Sherbrooke: Sherbrooke, QC, Canada, 2013. Available online: https://www.sadl.qc.ca/wp-content/uploads/2016/01/Rapport-final-Strategie_milieu-humides2.pdf (accessed on 22 December 2022).
38. ABVLACS (Agence des Bassin Versants de Sainte-Anne-des-Lacs). 2018. Available online: <http://abvlacs.org/lac-johanne/> (accessed on 22 December 2022).
39. MELCC—Ministère de l'Environnement et de la Lutte Contre les Changements Climatiques, 2018. Réseau de Surveillance Volontaire des lacs—Lac Caron (0387A)—Suivi de la Qualité de l'eau. 2020. Available online: https://www.environnement.gouv.qc.ca/eau/rsvl/relais/fiches-bilans/2020/Caron,%20Lac_0387A_2020_SA_SU.html (accessed on 11 July 2021).

40. MDDEP—Ministère du Développement Durable, de l'Environnement et des Parcs, 2012. Portrait de la Qualité des Eaux de Surface au Québec 1999–2008, Québec, Direction du Suivi de L'état de L'environnement. Available online: <http://www.environnement.gouv.qc.ca/eau/portrait/eaux-surface1999-2008/intro.pdf> (accessed on 11 July 2021).
41. Zhang, C.; Feng, W.; Chen, H.; Zhu, Y.; Wu, F.; Giesy, J.P.; He, Z.; Wang, H.; Sun, F. Characterization and sources of dissolved and particulate phosphorus in 10 freshwater lakes with different trophic statuses in China by solution ^{31}P nuclear magnetic resonance spectroscopy. *Ecol. Res.* **2018**, *34*, 106–118. [[CrossRef](#)]

Disclaimer/Publisher's Note: The statements, opinions and data contained in all publications are solely those of the individual author(s) and contributor(s) and not of MDPI and/or the editor(s). MDPI and/or the editor(s) disclaim responsibility for any injury to people or property resulting from any ideas, methods, instructions or products referred to in the content.